Monotone Finite Volume Schemes for Diffusion Equations on Distorted Quadrilateral Meshes

Jing-yan Yue, Guang-wei Yuan and Zhi-qiang Sheng

***Abstract*—We construct a new monotone finite volume scheme for diffusion problem on distorted quadrilateral meshes, and the scheme also takes account of the geometric distortion of cells and changes of physical variables on each edge, moreover, a part of the mesh stencil is fixed. The new scheme is proved to be monotone, i.e. it preserves positivity of analytical solutions. Numerical results are presented to demonstrate the numerical performance of our new monotone scheme such as solution positivity-preserving, conservation, accuracy and efficiency on distorted meshes.**

***Index Terms*—Diffusion equation, finite volume scheme, monotonicity, polygonal meshes.**

I. Introduction

INVESTIGATING the numerical schemes with high accuracy and efficiency for diffusion equations on distorted meshes is very important in Lagrangian hydrodynamics and magnetohydrodynamics. It is well known that classical finite volume (FV) and finite element (FE) schemes may produce non-monotone solutions on general meshes and for full diffusion tensors ([2], [3], [12]). In [12], it is shown that a linear nine-point method cannot unconditionally satisfy the monotonicity criteria on arbitrary quadrilateral meshes when the discretization satisfies local conservation and exact linearity-preserving as well. Severe restrictive conditions on the geometry of meshes or diffusion coefficients are imposed for some known schemes to satisfy the monotonicity or the discrete maximum principle ([5], [9], [11]). To guarantee solution positivity on general meshes, two repairing techniques are introduced in [8] for linear finite element method, and in [16] a limiter method is applied for anisotropic diffusion problems.

A number of nonlinear methods have been proposed for diffusion equation ([1], [4], [6], [7], [14], [15], [19]). The monotone FV method developed in this article is based on a nonlinear two-point flux approximation scheme. The original idea belongs to C. Le Potier who proposes a nonlinear FV scheme for highly anisotropic diffusion operators on unstructured triangular meshes in [14]. It is shown that the scheme for parabolic equations is monotone only for sufficiently small time steps. The method of [14] is further developed and analyzed in [6] for steady-state diffusion problems on shape regular polygonal meshes and with a special choice of collocation points.

Manuscript received December 8th, 2014. This work is supported by the National Natural Science Foundation of China (11271054, 11171036, 11301033), the Science Foundation of CAEP (2014A0202010) and the Foundation of the National Key Laboratory of Science and Technology on Computational Physics.

National Key Laboratory of Science and Technology on Computational Physics, Institute of Applied Physics and Computational Mathematics, P.O. Box 8009-26, Beijing 100088, China

Jing-yan Yue: email: yue_jingyan@iapcm.ac.cn, Guang-wei yuan: email: yuan_guangwei@iapcm.ac.cn, Zhi-Qiang Sheng: email: sheng_zhiqiang@iapcm.ac.cn

In [19] a monotone scheme on star-shaped polygonal meshes is constructed for diffusion equations with full tensor diffusion coefficients, where an adaptive strategy of constructing discrete flux is proposed to guarantee monotonicity on distorted meshes. The basic idea is to choose appropriate cell-edge entering into the stencil of discrete flux, and the key ingredient of the strategy is that the normal direction is decomposed into a weighted combination of two auxiliary directions with the weights being non-negative. Thus the geometric distortion of cells is taken into account in the construction of discrete normal flux, and it's unnecessary to define special collocation points. However, the chosen cell-edges in designing discrete normal flux may not include the original edge on which the discrete normal flux is defined. Thus, the physical variables on the original cell-edge cannot appear directly in the expression of the discrete flux.

Using characteristic of quadrilateral cells, we introduce a new design of monotone scheme for diffusion problem on distorted quadrilateral meshes. The scheme preserves solution positivity and conservation, and has high computational efficiency and it also takes account of the geometric distortion of cells and changes of physical variables on each edge. Moreover the new scheme keeps the same good merits of the scheme in [19].

The outline of this article is as follows. In section 2 we describe the construction of the new nonlinear monotone scheme. The numerical results are presented in section 3 to illustrate the basic features of the new scheme such as positivity, accuracy, discrete conservation and efficiency. Finally the conclusions are given in section 4.

II. Construction of monotone nonlinear scheme

A. Problem and notation

Let Ω be an open bounded polygonal set of R^2 with boundary $\partial\Omega$. Consider the stationary diffusion problem for unknown $u = u(x)$:

$$-\nabla \cdot (\kappa \nabla u) = f \quad in \ \Omega, \tag{1}$$

$$u(x) = g \quad on \ \partial\Omega, \tag{2}$$

where $\kappa = \kappa(x)$ is a positive definite matrix (possibly anisotropic), and $f = f(x)$ is a source term.

A discretization of Ω, denoted by $\mathcal{D}$, is given by $\mathcal{D} = (\mathcal{J}, \mathcal{E})$, where:

- $\mathcal{J} = \{K\}$ is a finite family of non-empty connected open disjoint subsets of Ω (the control volumes) such that $\overline{\Omega} = \cup_{K \in \mathcal{J}} \overline{K}$. For $K \in \mathcal{J}$, let ∂K denote the cell boundary.
- $\mathcal{E} = \{\sigma\}$ is a finite family of disjoint edges in $\overline{\Omega}$ (the edges of the mesh) such that for $\sigma \in \mathcal{E}$, σ is a line segment with a strictly positive length denoted by $|\sigma|$. We assume that, for all $K \in \mathcal{J}$, there exists a subset $\mathcal{E}_K$

ISBN: 978-988-19253-2-9
ISSN: 2078-0958 (Print); ISSN: 2078-0966 (Online)

of $\mathcal{E}$ such that $\partial K = \cup_{\sigma\in\mathcal{E}_K}\overline{\sigma}$. We also assume that, for all $\sigma \in \mathcal{E}$, either $\sigma \in \partial\Omega$ or $\sigma = K|L$ for some $(K, L) \in \mathcal{J}\times\mathcal{J}$. Let $\mathcal{E}_{int} = \mathcal{E}\cap\Omega$ and $\mathcal{E}_{ext} = \mathcal{E}\cap\partial\Omega$.

With each cell K we associate one point (the so-called collocation point or cell center) denoted also by K: the centroid is a qualified candidate. We assume that each cell is star-shaped with respect to the collocation point, that is any ray emanating from the cell center K intersects the boundary of cell K at exactly one point. All convex polygons are star-shaped. We assume $\kappa(x)$ is smooth piecewise with possible jump on the edges of mesh, so does the solution $u(x)$.

We use the following notations. Denote the cell vertex by A, B or $P_i, i = 1, 2, 3, \cdots$. $m(K)$ is the measure of cell K. Denote $h = \left(\sup_{K\in\mathcal{J}} m(K)\right)^{1/2}$. $\vec{n}_{K,\sigma}$ (resp. $\vec{n}_{L,\sigma}$) is the unit outer normal on the edge σ of cell K (resp. L). There holds $\vec{n}_{K,\sigma} = -\vec{n}_{L,\sigma}$ for $\sigma = K|L$. $\vec{t}_{KP_i}$ and $\vec{t}_{LP_i}$ are the unit tangential vectors on the line KP_i and LP_i ($i = 1, 2, \cdots$), respectively.

B. Construction of scheme

Integrate (1) over the cell K, to obtain

$$\sum_{\sigma\in\mathcal{E}_K}\mathcal{F}_{K,\sigma} = \int_K f(x)dx, \tag{3}$$

where the continuous flux on the edge σ is

$$\begin{aligned}\mathcal{F}_{K,\sigma} &= -\int_\sigma \kappa(x)\nabla u(x)\cdot\vec{n}_{K,\sigma}dl \\ &= -\int_\sigma \nabla u(x)\cdot\kappa(x)^T\vec{n}_{K,\sigma}dl,\end{aligned} \tag{4}$$

and $\kappa(x)^T$ is the transpose of matrix κ, and $\kappa(x)^T = \kappa(x)$.

A quadrilateral cell has the following characteristic: the geometrical center (Fig. 1) is the intersection point of two line segments that connect the midpoints of the opposite edges. Here we consider anisotropic problems and use the above characteristic to specially choose a kind of discrete stencil on quadrilateral meshes.

Since the matrix κ is positive definite, the ray originated in the point K along the direction of the co-normal vector $\vec{l}_{K,\sigma} = \kappa_K^T\vec{n}_{K,\sigma}$ must intersect the edge σ or the extension of σ, and the cross point is denoted by O_1 (Figs. 2, 3 and 4). Similarly, the ray originated in the point L along the direction $\vec{l}_{L,\sigma} = \kappa_L^T\vec{n}_{L\sigma}$ must intersect the edge σ or the extension of σ, and the cross point is O_2. For $\vec{a} = (a_1, a_2)$ and $\vec{b} = (b_1, b_2)$, we define $\vec{a}\odot\vec{b} = a_1b_2 - a_2b_1$ in this paper. There are three cases of the cross point's location:

1) The cross point is on the line segment σ (Fig. 2), i.e. $\vec{t}_{KB}\odot\vec{l}_{K,\sigma} \geq 0, \vec{l}_{K,\sigma}\odot\vec{t}_{KA} \geq 0$. Let $S_1 = B$, $S_2 = A$.
2) The cross point is on the extension of σ, and $\vec{t}_{KB}\odot\vec{l}_{K,\sigma} > 0, \vec{l}_{K,\sigma}\odot\vec{t}_{KA} < 0$ (Fig. 3). Let $S_1 = \frac{3A+B}{4}$, S_2 be the midpoint of P_1P_2 which is the opposite side of σ.
3) The cross point is on the extension of σ, and $\vec{t}_{KB}\odot\vec{l}_{K,\sigma} < 0, \vec{l}_{K,\sigma}\odot\vec{t}_{KA} > 0$ (Fig. 4). Let S_1 be the midpoint of P_1P_2, $S_2 = \frac{A+3B}{4}$.

Similarly, we can define S_3, S_4 for the cell L.

Let θ_{K_1} be the angle between KS_1 and KO_1, θ_{K_2} the angle between KO_1 and KS_2, θ_{L_1} the angle between LS_3 and LO_2, and θ_{L_2} the angle between LO_2 and LS_4. Denote $\theta_K = \theta_{K_1} + \theta_{K_2}$, i.e., θ_K is the angle between KS_1 and KS_2, and $\theta_L = \theta_{L_1} + \theta_{L_2}$, i.e., θ_L is the angle between LS_3 and LS_4. From the positive definiteness of κ it follows that there hold

$$0 \leq \theta_{K_i}, \theta_{L_i} < \pi \ \ (i = 1, 2) \ \text{ and } \ 0 < \theta_K, \theta_L < \pi. \tag{5}$$

Since the two vectors $\vec{t}_{KS_1}$ and $\vec{t}_{KS_2}$ cannot be collinear. The trigonometric observation gives the following (see [19] for details):

From the definition of S_i ($1 \leq i \leq 4$) there exist positive numbers $\tilde{\alpha}_{K,\sigma}$ and $\tilde{\beta}_{K,\sigma}$ such that

$$\frac{\vec{l}_{K,\sigma}}{|\vec{l}_{K,\sigma}|} = \tilde{\alpha}_{K,\sigma}\vec{t}_{KS_1} + \tilde{\beta}_{K,\sigma}\vec{t}_{KS_2}, \tag{6}$$

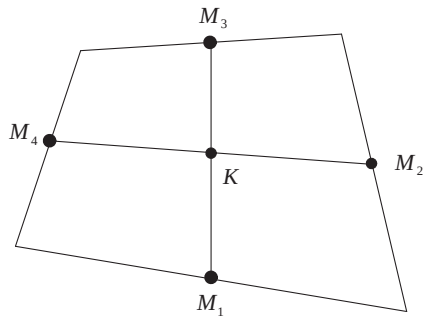

Fig. 1. Center of quadrilateral mesh

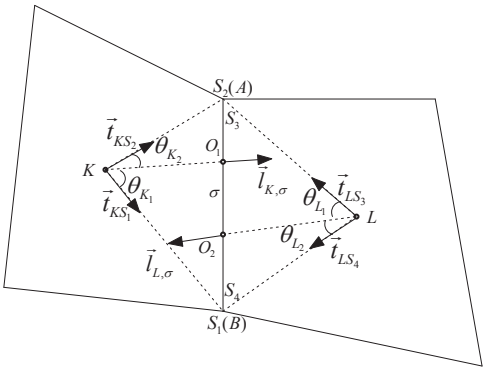

Fig. 2. Stencil for quadrilateral mesh 1

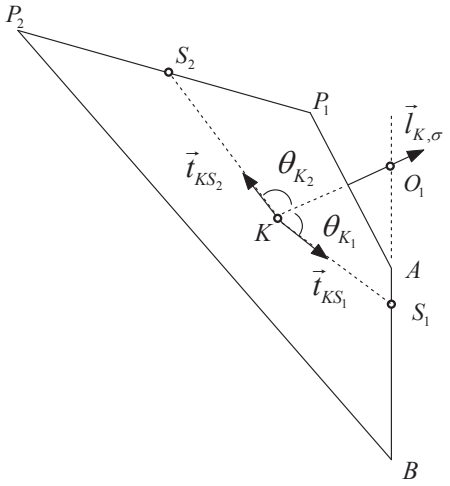

Fig. 3. Stencil for quadrilateral mesh 2

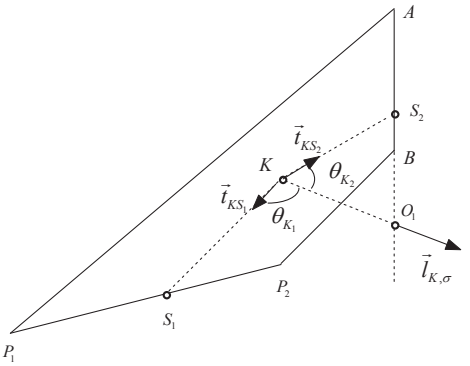

Fig. 4. Stencil for quadrilateral mesh 3

where

$$\tilde{\alpha}_{K,\sigma} = \frac{\sin\theta_{K_2}}{\sin\theta_K}, \tilde{\beta}_{K,\sigma} = \frac{\sin\theta_{K_1}}{\sin\theta_K}.$$

Similarly, there is

$$\frac{\vec{l}_{L,\sigma}}{|\vec{l}_{L,\sigma}|} = \tilde{\alpha}_{L,\sigma}\vec{t}_{LS_3} + \tilde{\beta}_{L,\sigma}\vec{t}_{LS_4}, \tag{7}$$

where

$$\tilde{\alpha}_{L,\sigma} = \frac{\sin\theta_{L_2}}{\sin\theta_L}, \tilde{\beta}_{L,\sigma} = \frac{\sin\theta_{L_1}}{\sin\theta_L}.$$

Substituting (6) into (4), we obtain

$$\begin{aligned}\mathcal{F}_{K,\sigma} &= -\int_\sigma |\vec{l}_{K,\sigma}|(\tilde{\alpha}_{K,\sigma}\nabla u(x)\cdot\vec{t}_{KS_1} \\ &+ \tilde{\beta}_{K,\sigma}\nabla u(x)\cdot\vec{t}_{KS_2})dl \\ &= -|\vec{l}_{K,\sigma}||\sigma|(\tilde{\alpha}_{K,\sigma}\frac{u(S_1)-u(K)}{|KS_1|} \\ &+ \tilde{\beta}_{K,\sigma}\frac{u(S_2)-u(K)}{|KS_2|}) + O(h^2).\end{aligned}$$

Let

$$F_1 = -|\vec{l}_{K,\sigma}||\sigma|\left(\tilde{\alpha}_{K,\sigma}\frac{u_{S_1}-u_K}{|KS_1|} + \tilde{\beta}_{K,\sigma}\frac{u_{S_2}-u_K}{|KS_2|}\right). \tag{8}$$

At the moment, this flux involves three rather than two unknowns. To derive a two-point flux on $\sigma = K|L$, we further consider the approximation of flux through edge σ of cell L as follows:

$$F_2 = -|\vec{l}_{L,\sigma}||\sigma|\left(\tilde{\alpha}_{L,\sigma}\frac{u_{S_3}-u_L}{|LS_3|} + \tilde{\beta}_{L,\sigma}\frac{u_{S_4}-u_L}{|LS_4|}\right). \tag{9}$$

Let $F_{K,\sigma}$ be the discrete normal flux on edge σ of cell K defined as a linear combination of F_1 and F_2 with non-negative coefficients μ_1 and μ_2:

$$\begin{aligned}F_{K,\sigma} &= \mu_1 F_1 - \mu_2 F_2, \\ &= \mu_1|\vec{l}_{K,\sigma}||\sigma|\left(\frac{\tilde{\alpha}_{K,\sigma}}{|KS_1|} + \frac{\tilde{\beta}_{K,\sigma}}{|KS_2|}\right)u_K \\ &\quad -\mu_2|\vec{l}_{L,\sigma}||\sigma|\left(\frac{\tilde{\alpha}_{L,\sigma}}{|LS_3|} + \frac{\tilde{\beta}_{L,\sigma}}{|LS_4|}\right)u_L \\ &\quad -\mu_1|\vec{l}_{K,\sigma}||\sigma|\left(\frac{\tilde{\alpha}_{K,\sigma}}{|KS_1|}u_{S_1} + \frac{\tilde{\beta}_{K,\sigma}}{|KS_2|}u_{S_2}\right) \\ &\quad +\mu_2|\vec{l}_{L,\sigma}||\sigma|\left(\frac{\tilde{\alpha}_{L,\sigma}}{|LS_3|}u_{S_3} + \frac{\tilde{\beta}_{L,\sigma}}{|LS_4|}u_{S_4}\right).\end{aligned} \tag{10}$$

where μ_1 and μ_2 are two numbers satisfying $\mu_1 + \mu_2 = 1$, and the last two rows of the above expression is required to be cancelled. Hence we choose μ_1 and μ_2 such that

$$\begin{cases} \mu_1 + \mu_2 = 1, \\ -a_1\mu_1 + a_2\mu_2 = 0, \end{cases} \tag{11}$$

where

$$\begin{aligned}a_1 &= |\vec{l}_{K,\sigma}||\sigma|\left(\frac{\tilde{\alpha}_{K,\sigma}}{|KS_1|}u_{S_1} + \frac{\tilde{\beta}_{K,\sigma}}{|KS_2|}u_{S_2}\right), \\ a_2 &= |\vec{l}_{L,\sigma}||\sigma|\left(\frac{\tilde{\alpha}_{L,\sigma}}{|LS_3|}u_{S_3} + \frac{\tilde{\beta}_{L,\sigma}}{|LS_4|}u_{S_4}\right).\end{aligned}$$

If $a_1 + a_2 \neq 0$, the solution of (11) is

$$\mu_1 = \frac{a_2}{a_1+a_2}, \qquad \mu_2 = \frac{a_1}{a_1+a_2}. \tag{12}$$

If $a_1 + a_2 = 0$, we set $\mu_1 = \mu_2 = \frac{1}{2}$.

The values a_1 and a_2 depend on both mesh geometry and physical unknowns, so do the coefficients μ_1 and μ_2 as well. Thus, the resulting two-point flux approximation is nonlinear.

From the definition of a_1 and a_1, we have

$$a_1 > 0, \qquad a_2 > 0,$$

provided that

$$u_{S_i} > 0, \quad i = 1,2,3,4, \tag{13}$$

which implies that

$$\mu_1 > 0, \qquad \mu_2 > 0.$$

For $\sigma = K|L \in \mathcal{E}_{int}$, by (10) and (11), we have

$$F_{K,\sigma} = A_{K,\sigma}u_K - A_{L,\sigma}u_L, \tag{14}$$

where

$$\begin{aligned}A_{K,\sigma} &= \mu_1|\vec{l}_{K,\sigma}||\sigma|\left(\frac{\tilde{\alpha}_{K,\sigma}}{|KS_1|} + \frac{\tilde{\beta}_{K,\sigma}}{|KS_2|}\right), \\ A_{L,\sigma} &= \mu_2|\vec{l}_{L,\sigma}||\sigma|\left(\frac{\tilde{\alpha}_{L,\sigma}}{|LS_3|} + \frac{\tilde{\beta}_{L,\sigma}}{|LS_4|}\right).\end{aligned}$$

Under the condition (13), it's obvious that there hold

$$A_{K,\sigma} > 0, \qquad A_{L,\sigma} > 0.$$

For $\sigma \subset \partial\Omega \cap \partial K$, we define

$$\begin{aligned}F_{K,\sigma} &= -|\vec{l}_{K\sigma}||\sigma|[\frac{\tilde{\alpha}_{K,\sigma}}{|KS_1|}u_{S_1} + \frac{\tilde{\beta}_{K,\sigma}}{|KS_2|}u_{S_2} \\ &\quad -\left(\frac{\tilde{\alpha}_{K,\sigma}}{|KS_1|} + \frac{\tilde{\beta}_{K,\sigma}}{|KS_2|}\right)u_K] \\ &= A_{K,\sigma}u_K - a_{K,\sigma},\end{aligned} \tag{15}$$

where

$$\begin{aligned}A_{K,\sigma} &= |\vec{l}_{K\sigma}||\sigma|\left(\frac{\tilde{\alpha}_{K,\sigma}}{|KS_1|} + \frac{\tilde{\beta}_{K,\sigma}}{|KS_2|}\right), \\ a_{K,\sigma} &= |\vec{l}_{K\sigma}||\sigma|\left(\frac{\tilde{\alpha}_{K,\sigma}}{|KS_1|}u_{S_1} + \frac{\tilde{\beta}_{K,\sigma}}{|KS_2|}u_{S_2}\right).\end{aligned}$$

ISBN: 978-988-19253-2-9
ISSN: 2078-0958 (Print); ISSN: 2078-0966 (Online)

With the definition of $F_{K,\sigma}$ the finite volume scheme is formulated as follows:

$$\sum_{\sigma\in\mathcal{E}_K} F_{K,\sigma} = f_K m(K), \qquad \forall K\in\mathcal{J}, \tag{16}$$

$$u_{P_i} = g_{P_i}, \qquad \forall P_i\in\partial\Omega, \tag{17}$$

where $f_K = f(K)$.

C. Discrete system and monotonicity theorem

Substituting (14) and (15) into (16), we get a nonlinear algebraic system

$$A(U)U = F, \tag{18}$$

where U is the vector of discrete unknowns at the collocation points and $A(U)$ is the matrix of this system. The matrix $A(U)$ is assembled from 2×2 matrices

$$A_\sigma(U) = \begin{pmatrix} A_{K,\sigma}(U) & -A_{L,\sigma}(U) \\ -A_{K,\sigma}(U) & A_{L,\sigma}(U) \end{pmatrix}$$

for interior edges and 1×1 matrices $A_\sigma(U) = A_{K,\sigma}(U)$ for Dirichlet edges. The vector F at the right hand of (18) is generated by the source and the boundary data.

The matrix $A(U)$ is non-symmetric and has the following properties:

1. All diagonal entries of matrix $A(U)$ are positive.
2. All off-diagonal entries of $A(U)$ are non-positive.
3. Each column sum in $A(U)$ is non-negative and there exists a column with a positive sum.

These properties implies $A(U)$ is weak diagonal dominance in column.

Just as [6], we use Picard iteration to solve the nonlinear system (18): Select an initial vector U^0 with non-negative entries and a small value $\varepsilon_{non} > 0$, and repeat for $k = 1, 2, \cdots,$

1. solve $A(U^{k-1})U^k = F$,
2. stop if $\|A(U^k)U^k - F\| \le \varepsilon_{non}\|A(U^0)U^0 - F\|$.

The linear system with non-symmetric matrix $A(U^{k-1})$ is solved by the GMRES method with ILUT preconditioner. The GMRES iterations are terminated when the relative norm of the residual becomes smaller than ε_{lin}.

In order to show that our schemes are monotone, we introduce the following theorem:

Theorem 1: For an irreducible matrix $A = (a_{ij})_{n\times n}$ satisfying $a_{ii} > 0 (1\le i\le n)$ and $a_{ij}\le 0$ ($1\le i,j\le n$, $i\ne j$), if A is weak diagonal dominance in rows, that is

$$\sum_{j=1}^{n} a_{ij} \ge 0 \qquad (i = 1, 2, \cdots, n), \tag{19}$$

with strict inequality for at least one of the equations (19). Then the matrix A is an M-matrix.

Then we claim that our scheme is monotone:

Theorem 2: Let $F\ge 0$, $U^0\ge 0$ and linear systems in Picard iterations are solved exactly. Then all iterates U^k are non-negative vectors:

$$U^k \ge 0.$$

Proof: We first prove that the matrix $A(U)$ is monotone for any vector U with non-negative components. In the above section, we have state some properties of matrix $A(U)$. It's obvious that the matrix $A^T(U)$ satisfies the conditions of theorem 1, hence $A^T(U)$ is an M-matrix, that is all entries of $(A^T(U)^{-1}$ are non-negative. Since inverse and transpose operation commute, $(A^T(U))^{-1} = (A^{-1}(U))^T$, we conclude that all entries of $A^{-1}(U)$ are non-negative and $A(U)$ is monotone for any vector $U\ge 0$.

Noticing that $U^0\ge 0$, we assume for some integer $k_0 > 0$,

$$U^{k_0-1}\ge 0.$$

Hence, the matrix $A(U^{k_0-1})$ is monotone, that is $A^{-1}(U^{k_0-1})\ge 0$. Also notice $F\ge 0$, it follows that the solution U^{k_0} of $A(U^{k_0-1})U^{k_0} = F$ is a non-negative vector, that is

$$U^{k_0}\ge 0.$$

By induction argument, there are

$$U^k\ge 0, \quad \text{for all} \quad k\ge 0.$$

■

III. Numerical experiments

When applying nonlinear schemes for solving linear diffusion problems the computational cost is usually high in comparison with a linear scheme. It is necessary to test the efficiency of nonlinear monotone scheme for solving nonlinear diffusion problems. Numerical results in this section will be given to demonstrate the performance of the new nonlinear scheme such as positivity-preserving, conservation and efficiency for the nonlinear system of equations for non-equilibrium diffusion coupled to material conduction ([10]):

$$\frac{\partial E}{\partial t} - \nabla\cdot(D\nabla E) = \sigma_a(T^4 - E), \tag{20}$$

$$\frac{\partial T}{\partial t} - \nabla\cdot(\kappa\nabla T) = \sigma_a(E - T^4), \tag{21}$$

where E is the radiation energy density, t time, D the radiation diffusion coefficient, T the material temperature, κ the material conduction coefficient, and σ_a the photon absorption cross section, which is modeled by

$$\sigma_a(T) = \frac{z^3}{T^3}. \tag{22}$$

In this model, z is a function of the material and varies as a function of space (x, y).

The radiation diffusion coefficient without flux limiter is as follows:

$$D = \frac{1}{3\sigma_a}. \tag{23}$$

In order to keep the propagation velocity of a radiation wave front in a vacuum less than the speed of light, one can use a flux-limited diffusion coefficient. We use the following form [13]:

$$D = \frac{1}{3\sigma_a + \frac{|\nabla E|}{E}}. \tag{24}$$

The material conduction coefficient κ has the following form

$$\kappa = c_0 T^{5/2}, \tag{25}$$

where $c_0 = 1.0\times 10^{-2}$.

ISBN: 978-988-19253-2-9
ISSN: 2078-0958 (Print); ISSN: 2078-0966 (Online)

The test problem (e.g., see [10]) is solved on the domain $\Omega = [0,1] \times [0,1]$. The value for z is 1 everywhere, except in the two obstacles defined by

$$\frac{3}{16} < x < \frac{7}{16}, \qquad \frac{9}{16} < y < \frac{13}{16},$$

and

$$\frac{9}{16} < x < \frac{13}{16}, \qquad \frac{3}{16} < y < \frac{7}{16},$$

where the value for z is 10. All four walls are insulated with respect to radiation diffusion and material conduction:

$$\left.\frac{\partial E}{\partial x}\right|_{x=0} = \left.\frac{\partial E}{\partial x}\right|_{x=1} = \left.\frac{\partial E}{\partial y}\right|_{y=0} = \left.\frac{\partial E}{\partial y}\right|_{y=1} = 0, \quad (26)$$

and

$$\left.\frac{\partial T}{\partial x}\right|_{x=0} = \left.\frac{\partial T}{\partial x}\right|_{x=1} = \left.\frac{\partial T}{\partial y}\right|_{y=0} = \left.\frac{\partial T}{\partial y}\right|_{y=1} = 0. \quad (27)$$

The initial radiation energy is given by

$$E(r) = 0.001 + 100 \exp\left[-\left(\frac{r}{0.1}\right)^2\right], \quad (28)$$

where $r = \sqrt{x^2 + y^2}$ is the distance from the origin, which is located in the lower left corner of the computational domain. The initial material temperature is equal to the radiation temperature

$$T(x,y) = E(x,y)^{1/4}.$$

From the boundary conditions (26) and (27), the total energy in the problem should be conserved. The total energy $\int_\Omega (E+T)dx$ is approximated by

$$E_{total} = \sum_{K \in \mathcal{J}} (E_K + T_K)\, m(K).$$

Denote E_{total}^{init} be the total energy at the initial state, E_{total}^{final} be the total energy at the final state, and E_{total}^{err} be the error of total energy between initial state and final state, that is

$$E_{total}^{err} = |E_{total}^{final} - E_{total}^{init}|.$$

In this subsection, we give the numerical results for the problem with flux limiter. We take $\Delta t = 5.0d-4$, and the final state $t = 3$.

First, we give the numerical results of our monotone scheme. The contours of the radiation temperature on rectangular and random quadrilateral meshes at $t = 3$ are shown in Figs. 5 and 6, respectively. Comparing these two figures, we see that the contours of the radiation temperature on random quadrilateral meshes accord with that on rectangular meshes. Moreover, the numerical solution on random quadrilateral meshes is positive in Ω. Table I gives the L_2-norm of solution on rectangular and random quadrilateral meshes. This table shows that the L_2-norm of solution on random quadrilateral meshes closely approximates to that on rectangular meshes.

TABLE I
L_2-NORM ON RECTANGULAR AND RANDOM QUADRILATERAL MESHES FOR THE PROBLEM WITH FLUX LIMITER

L_2 on rectangular meshes	L_2 on random quadrilateral meshes
1.1627	1.1624

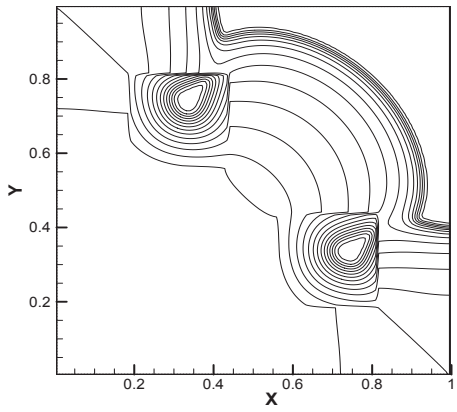

Fig. 5. The radiation temperature at $t = 3$ for the problem with flux limiter on rectangular meshes.

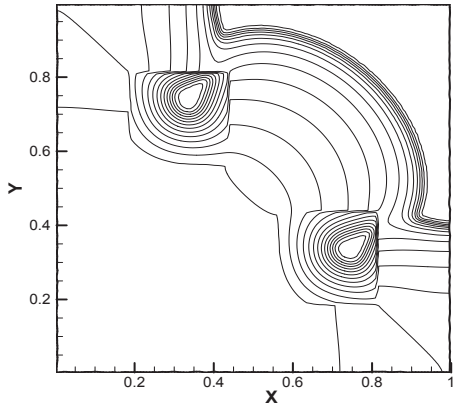

Fig. 6. The radiation temperature at $t = 3$ for the problem with flux limiter on random quadrilateral meshes.

Next, we compare the computational costs between the monotone scheme and the nine point scheme of [17]. A part of numerical solution is negative in the process of computation using nine point scheme which is not monotone. Because the negative solution will lead the breakdown of computation as the material conduction coefficient $\kappa_{K\sigma}$ is $c_0 T_{K\sigma}^{5/2}$, we replace the negative radiation energy density by 0.001 and the negative material temperature by $0.001^{1/4}$.

Table II gives the average numbers of nonlinear iterations and linear iterations on random quadrilateral meshes. We can see that the monotone scheme is more efficient than the nine point scheme for this problem.

TABLE II
THE AVERAGE NUMBER OF ITERATIONS FOR THE PROBLEM WITH FLUX LIMITER ON RANDOM QUADRILATERAL MESHES.

	Nonlinear iterations	Linear iterations
Monotone scheme	5.74	54.39
Nine point scheme	15.39	99.42

The conservation of total energy is one of the important features of the system for nonequilibrium radiation diffusion problem. Keeping the conservation is a key requirement for discrete schemes. We give the error of total energy between initial state and final state in Table III, which shows that

ISBN: 978-988-19253-2-9
ISSN: 2078-0958 (Print); ISSN: 2078-0966 (Online)

our monotone scheme is remarkably superior to nine point scheme in preserving the conservation of energy.

TABLE III
THE ERROR OF TOTAL ENERGY FOR THE PROBLEM WITH FLUX LIMITER ON RANDOM QUADRILATERAL MESHES.

	Monotone scheme	Nine point scheme
E_{total}^{err}	1.91E-7	9.86E-6

IV. CONCLUSION

In this article, we have developed a new nonlinear monotone finite volume method. In the construction of discrete normal flux on each cell-edge, both the geometric character of distorted cells and the physical variables on that cell-edge are taken into account. The scheme can be extended to three-temperature model, and 3D problem. Numerical experiments demonstrate the ability of preserving positivity of the new nonlinear scheme. Moreover, numerical test results indicate that our nonlinear monotone scheme is more efficient than the nine point scheme for solving nonlinear nonequilibrium radiation diffusion problem on quadrilateral meshes. It shows that our nonlinear monotone finite volume scheme is a practical method for solving nonlinear diffusion equations on distorted meshes.

REFERENCES

[1] E. Burman and A. Ern, Discrete maximum principle for Galerkin approximations of the Laplace operator on arbitrary meshes, C. R. Acad. Sci. Paris, Ser. I, 338:641-646, 2004.
[2] A. Draganescu, T. F. Dupont, and L. R. Scott, Failure of the discrete maximum principle for an elliptic finite element problem. Math. Comp., 74(249):1–23, 2004.
[3] H. Hoteit, R. Mose, B. Philippe, Ph. Ackerer, and J. Erhel, The maximum principle violations of the mixed-hybrid finite-element method applied to diffusion equations, Numer. Meth. Engng., 55(12):1373–1390, 2002.
[4] I. Kapyrin, A family of monotone methods for the numerical solution of three-dimensional diffusion problems on unstructured tetrahedral meshes, Doklady Mathematics, 76(2):734–738, 2007.
[5] S. Korotov, M. Krizek, and P. Neittaanmäki, Weakened acute type condition for tetrahedral triangulations and the discrete maximum principle. Math. Comp., 70:107–119, 2000.
[6] K. Lipnikov, M. Shashkov, D. Svyatskiy, and Yu. Vassilevski, Monotone finite volume schemes for diffusion equations on unstructured triangular and shape-regular polygonal meshes, J. Comput. Phys., 227:492–512, 2007.
[7] K. Lipnikov, D. Svyatskiy, and Yu. Vassilevski. Interpolation-free monotone finite volume method for diffusion equations on polygonal meshes, J. Comput. Phys., 228:703–716, 2009.
[8] R. Liska, and M. Shashkov, Enforcing the discrete maximum principle for linear finite element solutions of second-Order elliptic problems, Commun. Comput. Phys., 3:852-877, 2008.
[9] I. D. Mishev, Finite Volume methods on Voronoi meshes, Numerical methods for Partial Differential equations, 12(2):193–212, 1998.
[10] V. A. Mousseau and D. A. Knoll, Temporal Accuracy of the Nonequilibrium Radiation Diffusion Equations Applied to Two-Dimensional Multimaterial Simulations, Nuclear Science and Enginerring, 154:174–189, 2006.
[11] J. M. Nordbotten and I. Aavatsmark, Monotonicity conditions for control volume methods on uniform parallelogram grids in homogeneous media, Computational Geosciences, 9:61–72, 2005.
[12] J. M. Nordbotten, I. Aavatsmark and G. T. Eigestad, Monotonicity of control volume methods, Numer. Math., 106:255-288, 2007.
[13] G. L. Olson, L. H. Auer, and M. L. Hall, Diffusion, $P1$, and other approximate forms of radiation transport, J. Quant. Spectrosc. Radiat. Transfer, 64:619–634, 2000.
[14] C. Le Potier, Finite volume monotone scheme for highly anisotropic diffusion operators on unstructured triangular meshes. C. R. Acad. Sci. Paris, Ser. I, 341:787–792, 2005.
[15] C. L. Potier, Finite volume scheme satisfying maxcimum and minimum preinciples for anisotropic diffusion operators, in: R. Eymard, J.-M. H. (eds.) (Eds.), Finite Volumes for Complex Applications V, 103C118, 2008.
[16] Prateek Sharma and Gregory W. Hammett, Preserving monotonicity in anisotropic diffusion, J. Comput. Phys., 227:123–142, 2007.
[17] Z. Sheng and G. Yuan, A nine point scheme for the approximation of diffusion operators on distorted quadrilateral meshes, SIAM J. Sci. Comput., 30:1341–1361, 2008.
[18] Z. Sheng, J. Yue, and G. Yuan, Monotone finite volume schemes of nonequilibrium radiation diffusion equations on distorted meshes, SIAM J Sci Comput., 31:2915–2934, 2009.
[19] G. Yuan, and Z. Sheng, Monotone finite volume schemes for diffusion equations on polygonal meshes, J. Comput. Phys., 227:6288–6312, 2008.

ISBN: 978-988-19253-2-9
ISSN: 2078-0958 (Print); ISSN: 2078-0966 (Online)